AIP | Applied Physics Letters

The role of shear in the transition from continuous shear thickening to discontinuous shear thickening

Weifeng Jiang, Shouhu Xuan, and Xinglong Gong

Citation: Applied Physics Letters **106**, 151902 (2015); doi: 10.1063/1.4918344
View online: http://dx.doi.org/10.1063/1.4918344
View Table of Contents: http://scitation.aip.org/content/aip/journal/apl/106/15?ver=pdfcov
Published by the AIP Publishing

The role of shear in the transition from continuous shear thickening to discontinuous shear thickening

Weifeng Jiang, Shouhu Xuan, and Xinglong Gong[a)]
CAS Key Laboratory of Mechanical Behavior and Design of Materials, Department of Modern Mechanics, University of Science and Technology of China (USTC), Hefei 230027, China

(Received 20 March 2015; accepted 2 April 2015; published online 14 April 2015)

Dense non-Brownian suspension has rich rheology and is hard to understand, especially for distinguishing continuous shear thickening (CST) from discontinuous shear thickening (DST). By studying the shear stress dependent rheology of a well-known DST suspension of cornstarch in water, we find that the transition from CST to DST could occur not only by increasing the volume fraction ϕ but also by increasing the shear stress σ. For the recovery process of jammed suspension, we observe that the shear activates the time-dependent nature of particle rearrangement. DST can then be interpreted as the consequence of shear-induced jamming. Based on the test data, we plot the schematic phase diagram in the ϕ-σ plane and find out that ϕ and σ perform almost the same effect on flow-state transition. © *2015 AIP Publishing LLC*. [http://dx.doi.org/10.1063/1.4918344]

Suspension is a heterogeneous mixture, which is usually prepared by mixing solid particles into a Newtonian liquid. This dense particle suspension often exhibits shear thickening behavior thus its viscosity increases with shear rate.[1,2] The counterintuitive behavior attracts fundamental interest and has many practical applications such as damping, hip padding system, and body armor.[3,4] The formation of hydroclusters has been proposed to describe the microscopic origination for shear thickening of colloidal suspensions.[3,5] Particles are pushed forward each other by the applied shear field. Above a critical shear rate, particles are driven into close proximity and form the clusters. Because the particle concentration is higher in the cluster, the energy dissipation or viscosity increases.

For the large particles (diameter larger than 4 μm), the influence of the Brownian motion is abated, and the particles touch easily. According to the mechanism of the lubricated contacts between particles, the flow transits from lubrication to frictional contacts as the shear rate reaches a critical value. Then the friction coefficient immediately increases by orders of magnitude. As the friction coefficient varies from near-zero (hydrodynamic) to a certain value (boundary), the jamming density decreases accordingly.[6,7] When the volume fraction ϕ exceeds the jamming volume fraction in the boundary regime ϕ_{max}^{HD}, the system is jammed and forms force networks. In such case, the interparticle contacts play an important role to support the most applied stress[6,8–10] which is far beyond the range of lubrication stress.[2,11] In a standard rheology experiment, the shear stress or viscosity appears discontinuous jump in the shear thickening regime. This phenomenon is defined as discontinuous shear thickening (DST). Otherwise, when $\phi < \phi_{max}^{HD}$, the suspension is in the boundary regime. It is equivalent to a dense dry granular flow and fits with a Bagnoldian scaling ($\tau \propto \dot{\gamma}^2$). This causes a gentle viscosity increase at any shear rate, which is defined as continuous shear thickening (CST).[6,9]

This mechanism explains some key puzzles for dense non-Brownian suspensions, such as the onset of shear thickening, the distinction between CST and DST, and the existence of normal force. More significantly, this mechanism suggests that the liquid-solid transition in DST suspension is a jamming transition and provides a new solution from the jamming field for describing the DST response. Jamming of gains has been widely studied in the past. It is now commonly accepted that the applied shear stress can induce the jamming of frictional gains at the density lower than the random close packing ϕ_{RLP}, at which shear-free jamming occurs.[12,13] In the terms of dense non-Brownian suspensions, the role of shear in DST response is poorly understood, but significantly important to understand the origin of the DST.

In this letter, we study the rheology of a well-known DST suspension of cornstarch in water under various shear stresses. With increasing of the shear stress, the DST suspension exhibits Newtonian (Nw), CST, DST (in terms of shear jamming (SJ)), and yield (in terms of unjamming (UJ)) states. Our findings show that the CST-DST transition occurs in term of both of volume fraction and shear. Moreover, the role of shear on the flow state transitions in the DST suspension was discussed, and the microscopic origin of the flow states was proposed.

Here, a dense suspension of cornstarch particles in water was prepared and its rheological properties were analyzed. The cornstarch particles (average particle diameter of 40 μm, *Sigma Aldrich*) suspension, with density matched to 1.59 g/ml, were measured by using a torque rheometer (Anton Paar, Physica MCR301) with thickness of 0.6 mm. Sandpaper was glued on the plate surface to avoid wall slip and the measurements with different gap sizes were performed to check the slip. No significant differences were found, so the wall slip could be ignored. The suspension was placed in a sealed chamber to prevent evaporation. A pre-shear schedule was used to provide consistent flow.

Fig. 1(a) shows viscosity vs shear rate traces for different volume fractions. For the 33% suspension, the viscosity slowly increases as the increase of shear rate, exhibiting CST

[a)]Electronic mail: gongxl@ustc.edu.cn

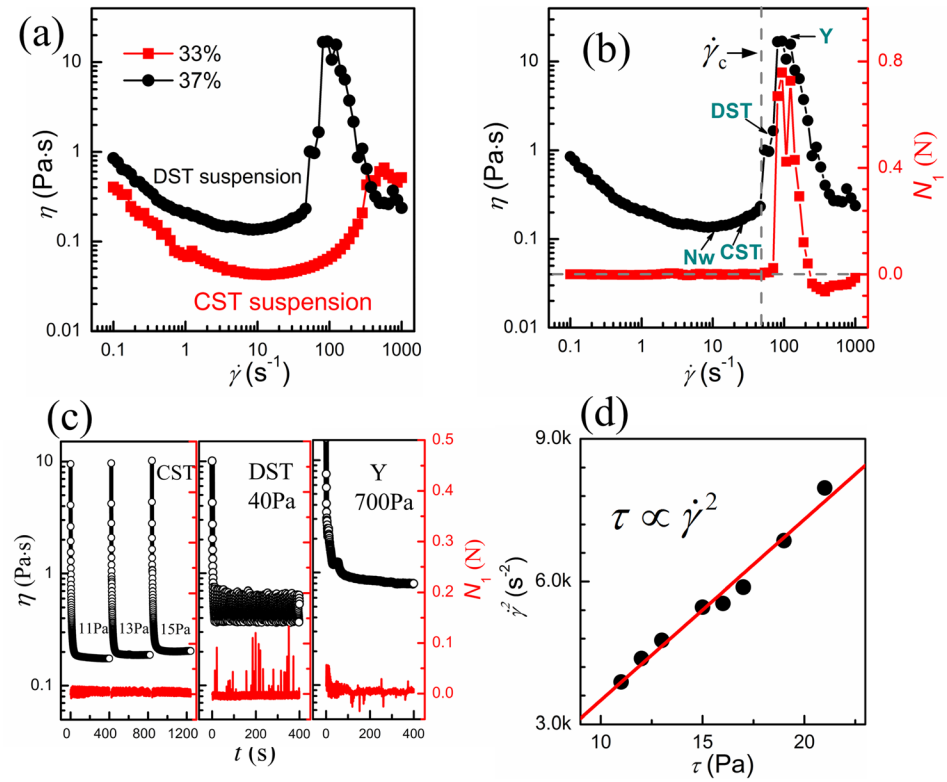

FIG. 1. (a) Viscosity η versus shear rate $\dot{\gamma}$ for various volume fractions. (b) Viscosity η and normal force N_1 versus shear rate $\dot{\gamma}$ for a 37% suspension. Before the Nw flow, the suspension exhibit shear thinning response. It disappears when the suspension is density matched. The detailed results for this phenomenon are discussed in detail in Refs. 14 and 15. (c) Viscosity η and normal force N_1 versus time t for various shear stresses σ when shearing a 37% suspension. In the first few seconds, the viscosity is large. It is due to the gravity that particle sedimentation develops well. During the shear, the sedimentary particles start moving, and particle distribution of the system becomes ordered, which causes the decreasing of the apparent viscosity. (d) Square of the shear rate versus shear stress. The red line is a linear-law with a slope of 380.6.

response. For the 37% suspension, the viscosity sharply increases as the increase of shear rate, exhibiting DST response. This result implies that the transition from CST to DST can occur by increasing the volume fraction. To distinguish the shear dependency flow state of the DST suspension, the normal force which identifies the formation of the force networks is measured (Fig. 1(b)). Along the $\dot{\gamma}$ axis, there are two states: below $\dot{\gamma}_c$ normal force approximates to zero and the system is unjamming, and above $\dot{\gamma}_c$ normal force appear and the system is jamming. The suspension exhibits Nw, CST, DST, and yield states as the shear stress increases. This implies that the transition from CST to DST does not occur only by increasing the volume fraction but also by increasing the shear stress. It is clear that the shear-induced frictional contacts between particles are the microscopic origin for the CST. This suggests that besides the frictional contact, some other conditions are necessary for the onset of DST. To clarify this, we focus on the rheology under fixed shear stress. Fig. 1(c) shows the time dependency of viscosity and normal force for a 37% DST suspension for different shear stresses. At lower shear stresses of 11, 13, and 15 Pa, their viscosities gradually approach a constant value. The viscosity mildly increases with the increasing of shear stress and the suspension fits a Bagnoldian scaling (Fig. 1(d)). These results imply that the CST response occurs in the DST suspension.[16] When the shear stress reaches 40 Pa, the viscosity appears periodical oscillation. Intuitively, the velocity of the plate exhibits stop-go oscillations.[17] The normal force appears when the suspension is jammed. These behaviors can be explained as follows. The system becomes solid-like when a load is beyond the critical shear stress or the corresponding shear rate (one-to-one correspondence between shear stress and shear rate before shear thickening). At the same time, the shear rate declines immediately. The DST response cannot occur in this case, so the system backs to liquid-like gradually. The evolution processes of the viscosity are shown in Fig. 2(a). Under the constant shear stress, the jamming (becoming solid-like) and relaxation (going back to liquid-like) states switch periodically throughout time and the jamming happens when the viscosity relaxes to the value $\eta_c = \tau/\dot{\gamma}_c$, where $\dot{\gamma}_c$ is critical shear rate for the onset of DST. When the stress reaches 700 Pa, the viscosity returns to a fixed value. The normal force fluctuates in a tight range near the zero point. These results suggest that the stable force network cannot be formed when the applied stress is beyond a critical value (yield stress). The suspension is unjammed and thus presents in a liquid-like state.

The notable behavior of the relaxation is that solid-like state relaxes back to liquid-like state after a certain time, indicating the time-dependent nature of the refactoring of the particle configuration. The DST suspension viscosity relaxation is mainly manifested in the particles of movement and rearrangement. Moreover, this behavior can be regarded as a process that the system recovers from the jammed state to the unjammed state. Therefore, it is closely related the formation of jamming response and can be used to study the origin of DST. We fit the traces to a power-exponent law as shown in the following equation:

$$\eta(t) = \eta_{j-r} e^{-t_r/t} + \eta_r, \tag{1}$$

where η_r is defined as the viscosity when the suspension relaxes completely and equals $\eta(t = \infty)$; η_j is defined as the viscosity when the suspension jams and equals $\eta(0)$; η_{j-r} equals $\eta_j - \eta_r$; and t_r is defined as the relaxation time and equals $\eta_{j-r}/\dot{\eta}_{t=0}$. As show in Fig. 2(a), the trend of the fitted line reflects quite well the viscosity relaxation process. The

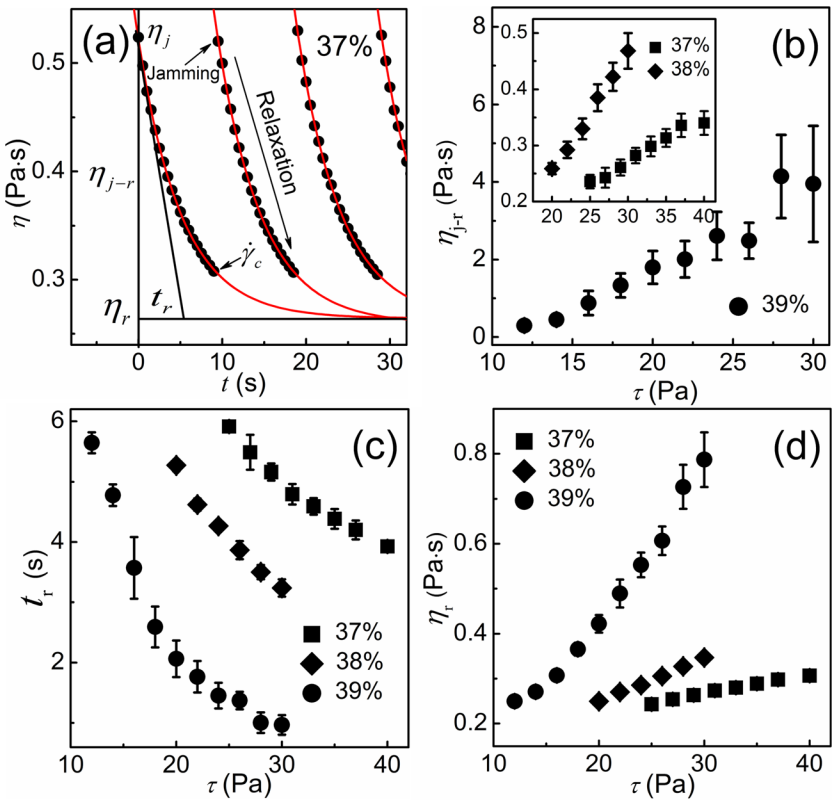

FIG. 2. (a) Apparent viscosity η versus time t for a 37% suspension at shear stress of 29 Pa. The red solid line is a power-exponent fit. Fitting parameters (b) viscosity η_{j-r}, (c) relaxed viscosity η_r, and (d) relaxation time t_r versus shear stress σ for the volume fractions of 37%, 38%, and 39%, respectively. Note that the 39% suspension is near the shear-free jamming. This causes the big error in its parameters. We focus in the following on the behavior of 37% and 38% suspensions.

parameters η_{j-r}, η_r, and t_r are shown in Figs. 2(b)–2(d), respectively, and exhibit shear stress dependence. Fig. 3(a) shows a linear relationship between the square of the relaxation shear rate $\dot{\gamma}_r{}^2$ ($\dot{\gamma}_r = \tau/\eta_r$) and the shear stress τ for two different volume fractions. It is similar to the behavior of CST flow and the viscosity is stabilized on the value of η_r. This establishes that the force network cannot be formed even under the high shear stress when the system has enough time to adjust the particle configuration. Otherwise, the system is jammed and exhibits DST response as shown in Fig. 3(b) ($\tau \propto \eta_j$). In the following, we focus on the behavior of the time-dependent jammed viscosity. The relaxation time t_r decreases as the shear stress increases (see Fig. 2(c)). This is probably due to the shear stress expediting the rearrangement of the particles. Fig. 3(c) shows a plot of the jammed viscosity versus relaxation time for two different volume fractions. The jammed viscosity decreases as the relaxation time increases. The result indicates that the shear can activate the time-dependent nature of the particles rearrangement and can distinguish the CST (occurring at low shear rate) and DST (occurring at high shear rate). According to the above conclusions, the picture of the evolution of the microstructure emerges and helps us to understand the origin of DST. If shear rate is low enough, the forced nearby particles have enough time to relax the particle configuration to the equilibrium state. However, at high shear rate, the particles touch with each other and have no time to separate. When the encounter particles propagate through the whole system, the shear-jammed contact network is formed. In this case, the system requires more spaces to adjust the jammed configuration. Therefore, dilatancy is often observed along with the DST.[16]

It can be found that the phase transition of the DST suspension was affected by the shear. Based on the above analysis, a schematic phase diagram in the ϕ-τ plane can be proposed (Fig. 4). For $\tau < \tau_j$, the viscosity is constant under the fixed shear stress. The system exhibits two kinds of flow state, including Nw flow and CST flow. If there is no yield

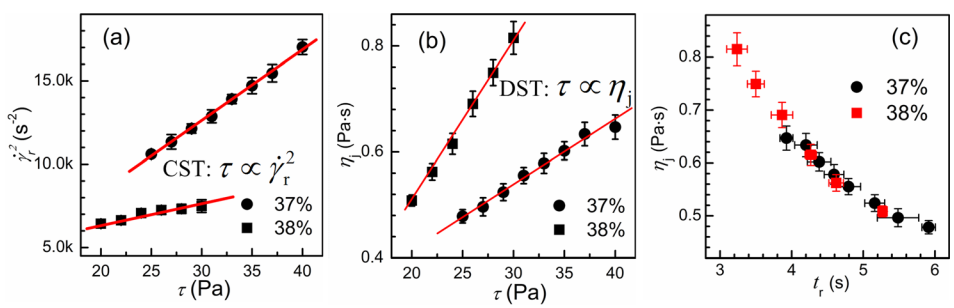

FIG. 3. (a) Square of the relaxation shear rate $\dot{\gamma}_r{}^2$ versus shear stress τ for the volume fractions of 37%, 38% and $\dot{\gamma}_r = \tau/\eta_r$. The red line is a linear-law fit to the volume fraction of 37% with a slope of 425.6, and the volume fraction of 38% with a slope of 108.4. (b) Jammed viscosity η_j versus shear stress τ for the volume fractions of 37% and 38%. The red line is a linear-law fit to the volume fraction of 37% with a slope of 0.012, and the volume fraction of 38% with a slope of 0.031. (c) Jammed viscosity η_j versus relaxation time t_r for the volume fractions of 37% and 38%.

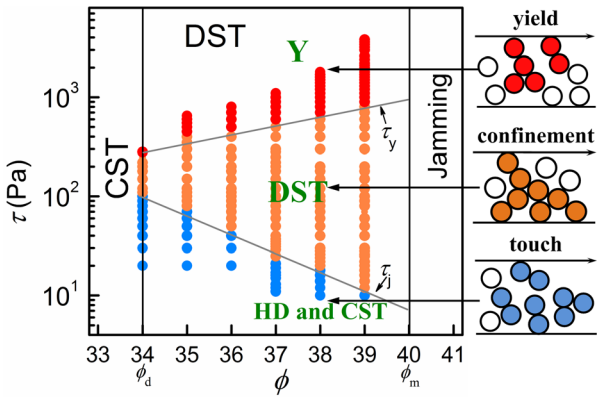

FIG. 4. Jamming phase diagram for dense non-Brownian suspension. Along the ϕ axis, there are two critical densities: ϕ_d, below which CST is found, and $\phi_m = \phi_{RLP}$, above which the suspension is solid-like in the normal. For $\phi_d < \phi < \phi_m$, shear jamming can occur with application of the shear stress.

stress in the suspension,[18,19] the particles do not contact each other and the system is in the lubrication state. In this case, the viscosity is independent of shear rate (Nw flow). With further increasing of the shear rate, the flow state transits from lubrication to frictional contacts. The particles become contacts to with each other, without forming the jammed contact network. Due to the particle-particle collisions, there is wastage of energy, and the viscosity increases ($\tau \propto \dot{\gamma}^2$). Experimentally, CST response is found. These states were referred as "hydrodynamic regime (HD) and CST." As τ increases above τ_j, SJ occurs. τ_j decreases as ϕ increases. In this case, the force network percolates in the whole system. For $\tau \geq \tau_y$, UJ occurs. τ_y increases as ϕ increases. At this point, the viscosity reaches to a maximum value $\eta_{max} = \tau_y/\dot{\gamma}_c$. In this case, the applied shear stress exceeds the particles interaction stress. The system is not able to form the stable force chain. Another notable feature in Fig. 4 is that ϕ_d and ϕ_m for cornstarch suspensions are smaller than these for glass suspensions or polymer-grafted sphere suspensions ($\phi_d \cong 58\%$).[6,17] That is because the attractive interactions between particles have the same effect in jamming system as the volume friction. In the suspension, the forces could be caused by Brownian motion,[20,21] friction,[6,9,10,22] polymer bridging,[23] etc. The stronger the attractive interaction, the smaller the critical volume fraction at which the isotropic jamming or shear thickening occurs.[24,25]

In conclusion, we have shown that the shear plays an important role in the flow-state transition of the DST suspension. For τ litter lower than τ_j, the CST response occurs and causes by the shear-induced particle contacts. For $\tau_j \leq \tau < \tau_y$, the DST occurs at volume fractions smaller than the random close packing and is ascribed to the shear-induced jamming. For $\tau \geq \tau_y$, the DST suspension becomes liquid-like again and causes by shear-induced fragmentation of the force chain. Notably, shear-induced jamming in DST suspension may be connected to the recent observations in dry granular materials.[9,12] It shows that application of shear to an unjammed state in ϕ lower than ϕ_{RLP} leads to force network. However, the difference is that the onset of shear jamming for dry granular materials is the shear strain, but the onset of shear jamming for DST suspension is the shear rate. The natural connection of these two phenomena should be further studied.

Financial supports from the National Natural Science Foundation of China (Grant Nos. 11372301 and 11125210), the National Basic Research Program of China (973 Program, Grant No. 2012CB937500), and the Anhui Provincial Natural Science Foundation of China (140805QA17) are gratefully acknowledged. This work was supported by Collaborative Innovation Center of Suzhou Nano Science and Technology.

[1]H. A. Barnes, J. Rheol. **33**, 329 (1989).
[2]E. Brown and H. M. Jaeger, Rep. Prog. Phys. **77**, 046602 (2014).
[3]N. J. Wagner and J. F. Brady, Phys. Today **62**(10), 27 (2009).
[4]Y. S. Lee, E. D. Wetzel, and N. J. Wagner, J. Mater. Sci. **38**, 2825 (2003).
[5]X. Cheng, J. H. McCoy, J. N. Israelachvili, and I. Cohen, Science **333**, 1276 (2011).
[6]N. Fernandez, R. Mani, D. Rinaldi, D. Kadau, M. Mosquet, H. Lombois-Burger, J. Cayer-Barrioz, H. J. Herrmann, N. D. Spencer, and L. Isa, Phys. Rev. Lett. **111**, 108301 (2013).
[7]C. Song, P. Wang, and H. A. Makse, Nature **453**, 629 (2008).
[8]R. Seto, R. Mari, J. F. Morris, and M. M. Denn, Phys. Rev. Lett. **111**, 218301 (2013).
[9]M. Wyart and M. E. Cates, Phys. Rev. Lett. **112**, 098302 (2014).
[10]J. R. Melrose and R. C. Ball, J. Rheol. **48**, 961 (2004).
[11]S. R. Waitukaitis and H. M. Jaeger, Nature **487**, 205 (2012).
[12]D. Bi, J. Zhang, B. Chakraborty, and R. P. Behringer, Nature **480**, 355 (2011).
[13]J. Ren, J. A. Dijksman, and R. P. Behringer, Phys. Rev. Lett. **110**, 018302 (2013).
[14]A. Fall, N. Huang, F. Bertrand, G. Ovarlez, and D. Bonn, Phys. Rev. Lett. **100**, 018301 (2008).
[15]A. Fall, F. Bertrand, G. Ovarlez, and D. Bonn, Phys. Rev. Lett. **103**, 178301 (2009).
[16]A. Fall, F. Bertrand, D. Hautemayou, C. Mezière, P. Moucheront, A. Lemaître, and G. Ovarlez, Phys. Rev. Lett. **114**, 098301 (2015).
[17]S. von Kann, J. H. Snoeijer, and D. van der Meer, Phys. Rev. E **87**, 042301 (2013).
[18]E. Brown and H. M. Jaeger, Phys. Rev. Lett. **103**, 086001 (2009).
[19]E. Brown, N. A. Forman, C. S. Orellana, H. Zhang, B. W. Maynor, D. E. Betts, J. M. DeSimone, and H. M. Jaeger, Nat. Mater. **9**, 220 (2010).
[20]V. Gopalakrishnan and C. F. Zukoski, J. Rheol. **48**, 1321 (2004).
[21]E. Brown and H. M. Jaeger, J. Rheol. **56**, 875 (2012).
[22]R. Mari, R. Seto, J. F. Morris, and M. M. Denn, J. Rheol. **58**, 1693 (2014).
[23]M. Kamibayashi, H. Ogura, and Y. Otsubo, J. Colloid Interface Sci. **321**, 294 (2008).
[24]V. Trappe and D. A. Weitz, Phys. Rev. Lett. **85**, 449 (2000).
[25]V. Trappe, V. Prasad, L. Cipelletti, P. N. Segre, and D. A. Weitz, Nature **411**, 772 (2001).